Insect Biochemistry and Molecular Biology 108 (2019) 1–8

Contents lists available at ScienceDirect

Insect Biochemistry and Molecular Biology

journal homepage: www.elsevier.com/locate/ibmb

Intersex regulates female external genital and imaginal disc development in the silkworm

Jun Xu[1], Ye Yu[1], Kai Chen, Yongping Huang[*]

Key Laboratory of Insect Developmental and Evolutionary Biology, Institute of Plant Physiology and Ecology, Shanghai Institutes for Biological Sciences, Chinese Academy of Sciences, Shanghai, 200032, China

ARTICLE INFO

Keywords:
Genome editing
Female external genital
Imaginal disc
Intersex
Bombyx mori

ABSTRACT

As a component of the mediator complex, the *intersex* (*ix*) gene product is involved in the sex determination pathway of the *Drosophila melanogaster*. IX functions together with the female-specific product of *doublesex* (*dsx*) at the bottom of the hierarchy to implement female sexual differentiation. Here we analyzed the functions of the *ix* gene in the model lepidopteran insect *Bombyx mori*. We found that *Bmix* is expressed in many tissues and is highly expressed in early pupal stages. We used the transgene-based CRISPR/Cas9 system to generate mutants of the *Bmix* gene. The *Bmix* female mutants were sterile and had irregular external genitalia, whereas in the mutant males external genitalia were normal. Mutants of both sexes had normal gonad development and normal splicing of the *Bmdsx* pre-mRNA, suggesting that *Bmix* functions independently of *Bmdsx*. Interestingly, both male and female mutants had defective development of the imaginal disc including wing, antenna, and leg. RNA-seq and gene expression analyses indicated that genes involved in WNT, Hippo, and Hedgehog signaling pathways and wing development genes *Bmawd* and *Bmfng* were up-regulated or down-regulated in the *Bmix* mutants compared with wild-type animals. Our data provide insights into the multiple functions of *Bmix* in female external genital and imaginal disc development in the silkworm.

1. Introduction

The primary signals in the genetics hierarchy of sex determination pathways are diverse among the Insecta. In the model organism, *Drosophila melanogaster*, the ratio of the X chromosome to the autosome is the primary signal for sex determination and the cascade involving *sex-lethal* (*Sxl*), *transformer* (*tra/tra2*), *doublesex* (*dsx*)/*intersex* (*ix*), *fruitless* (*fru*) controls development (Gempe and Beye, 2011; Erickson and Quintero, 2007; Graham et al., 2011; Hashiyama et al., 2011; Kappes et al., 2011; Vicoso and Bachtrog, 2013). Another dipteran, *Musca domestica*, employs *CWC22* as a dominant male determiner (Sharma et al., 2017). In *Aedes aegypti Nix* encodes the male-determining factor (M-factor) (Hall et al., 2015), whereas in *Anopheles gambiae* the male-determining factor is encoded by *Yob* (Krzywinska et al., 2016). These sex determination factors control the sex-specific splicing of *dsx*.

In the domesticated and economically important insect *Bombyx mori*, females possess a female-determining W chromosome and have heteromorphic sex chromosomes (ZW), and males are homomorphic (ZZ). The product of the W chromosome-derived *B. mori* sex determination factor *Fem*, which is the precursor of a PIWI-interacting RNA, is the primary female sex determinator (Kiuchi et al., 2014). Previous study showed the *B. mori* orthologues of the *Drosophila* genes *Sxl* and *tra2* genes do not function in sex determination in the silkworm (Suzuki et al., 2012; Xu et al., 2017a). Genetic evidence suggests that in the silkworm the sex determination cascade involves *Fem*, *Masc/PSI*, and *dsx* (Xu et al., 2017a; Sakai et al., 2016).

Although the upstream genes of sex determination pathway in insects are diverse, the genes *dsx* is conserved. Silkworm *Bmdsx* (Xu et al., 2014, 2017b), tribolium *Tcdsx* (Shukla and Palli, 2012), *Aedes Aadsx* (Mysore et al., 2015), and sawfly *Ardsx* (Mine et al., 2017) appear to function similarly to *Drosophila Dmdsx* to control sexual differentiation (Burtis and Baker, 1989). Although *ix* is conserved, the function has not been well characterized except in *D. melanogaster*. In *Drosophila*, IX is a subunit of the mediator complex, which functions with the products of *dsx* to control sex determination and differentiation (Garrett-Engele et al., 2002; Chatterjee et al., 2015). In the absence of *Dmix*, the female genital primordium does not differentiate. Data from a yeast two-hybrid assay and immunoprecipitation results suggest that there is a physical interaction between IX and DSX^F but not DSX^M (Garrett-Engele et al.,

* Corresponding author.
E-mail address: yphuang@sibs.ac.cn (Y. Huang).
[1] Contributed equally.

https://doi.org/10.1016/j.ibmb.2019.02.003
Received 21 December 2018; Received in revised form 12 February 2019; Accepted 25 February 2019
Available online 01 March 2019
0965-1748/

2002; Chatterjee et al., 2015; Siegal and Baker, 2005). Expression of dipteran and lepidopteran *ix* homologs, including those from silkworm and *Maruca vitrata*, partially restore sexual differentiation in *D. melanogaster* females lacking *ix* (Siegal and Baker, 2005; Cavaliere et al., 2009).

Although overexpression of the silkworm *Bmix* does not fully restore wild-type female development in the fly, the dorsal and ventral anal plates are present and appear normal (Siegal and Baker, 2005). This, and the finding that the *Bmix* gene has a testis-specific splice product suggest that there has been partial divergence of *ix* gene function between the *D. melanogaster* and *B. mori* (Arunkumar and Nagaraju, 2011). Here we used the binary transgenic CRISPR/Cas9 system to generate *Bmix* somatic mutations. We analyzed effects of mutations in *Bmix* on the sexually dimorphic traits of reproductive structures and on the sex-specific alternative splicing of *Bmdsx*. We found that *Bmix* is expressed in many tissues and is highly expressed in early pupal stages. Unlike the effects of loss of IX in *Drosophila*, both male and female *Bmix* mutants had normal gonad development and normal splicing of *dsx* pre-mRNA. We observed that female external genitals were affected. We also observed defects in development of wing imaginal disc at pupa stage in both male and female *Bmix* mutants and altered expression of genes involved in WNT, HIPPO, and HEDGEHOG signaling pathways and wing development relate genes *Bmawd* and *Bmfng*. These data strongly support the hypothesis that in *B. mori*, the *ix* gene product is important not only in differentiation of female external genital but also has multiple physiological functions during organ differentiation.

2. Materials and methods

2.1. Silkworm strains

The multivoltine, nondiapausing silkworm strain Nistari was used for all experiments. The larvae were reared on fresh mulberry leaves under standard conditions (Xu et al., 2017a). The transgenic strain *nos-Cas9*, which expresses the *Cas9* gene was previously described (Xu et al., 2017a). The transgenic strain *U6-BmixsgRNA* that expresses two single guide RNAs (sgRNAs) targeting *Bmix* under the control of the silkworm small nuclear RNA promoter U6 was constructed through a series of cloning steps. The sgRNA targets were selected by searching the *Bmix* genomic region for matches to the 5′-GG-N_{18}-NGG-3′ rule (Wang et al., 2013). sgRNA sequences were evaluated bioinformatically for potential off-target binding to the silkworm genome using CRISPRdirect (http://crispr.dbcls.jp/) (Naito et al., 2015). sgRNA sequences and sequences of oligonucleotide primers used for plasmid construction are listed in Table S1. The transgenic vector *pBac*[IE1-DsRed2-*U6-BmixsgRNA*] (referred to here as *U6-BmixsgRNA*) was obtained by microinjection of plasmid solutions into preblastoderm embryos followed by subsequent incubation and rearing. Putative transgenic G_0 adults were mated to wild-type (WT) moths, and the G_1 progeny were scored for the presence of the eye-specific or ubiquitous fluorescence marker using fluorescence microscopy (Nikon AZ100).

2.2. Mutagenesis analysis

Three U6-sgRNA transgenic lines were mated individually with the *nos-Cas9* line to derive F_0 animals. Genomic DNA was extracted at the embryonic or larval stage using standard SDS lysis-phenol treatment after incubation with proteinase K, followed by RNase treatment and purification. Gene amplification was performed using 50 ng of genomic DNA as the template. Mutation events were detected by amplification using gene-specific primers designed to hybridize upstream or downstream of the each target (Table S1). Amplified products were visualized by 2% agarose gel electrophoresis run 30 min at 100 V. Amplicons were sub-cloned into the pJET-1.2 vector (Fermentas), and four positive clones were sequenced.

2.3. Photography, scanning electron microscopy and paraffin sectioning

Wing discs of mutant or WT animals were dissected from larval stage insects and subjected to morphological investigation under a microscope (Nikon). External genitalia of the adults were photographed using a digital camera (Nikon DS-Ri1).

The dissected body segments and external genitalia were fixed overnight in Formalin-acetic acid-alcohol (FAA; 90 ml 70% ethanol, 5 ml acetic acid, 5 ml 37% methyl aldehyde), dehydrated in a series of 70%, 80%, 90%, and 100% ethanol (5 min each solution), and dried (under CO_2 for 6 h). The dissected materials were coated with gold and observed under a JEOL JSM-6360LV scanning electron microscope. The photographs are representative of samples obtained from three independent experiments.

Tissue sectioning was performed as described previously (Xu et al., 2017a). Gonads were dissected at the fourth day of the fifth instar stage and fixed in Qurnah's fixative (anhydrous ethanol: acetic acid: chloroform, 6:1:3 (v/v/v)) overnight. Sections were dehydrated and cleared three times using anhydrous ethanol and xylene. Tissues were embedded in paraffin overnight and sectioned using a Leica microtome (RM2235). Sections were stained using a mixture of hematoxylin and eosin to visualize morphology. All pictures were captured with an Olympus BX51 microscope using differential interference contrast and the appropriate filter.

2.4. Semi-quantitative RT-PCR

Total RNA was extracted from silkworm larvae using the Trizol reagent (Invitrogen) and treated with RNase-free DNase I (Ambion). The cDNAs were synthesized using the Omniscript Reverse transcriptase kit (Qiagen) in a 20-μl reaction mixture containing 1 μg of total RNA. RT-PCR reactions were carried out using KOD plus polymerase (Toyobo) with gene-specific primers (Table S1). Amplification of the gene encoding ribosomal protein 49 (*Bmrp49*) was used as a positive control.

2.5. Quantitative real-time RT-PCR

Quantitative real-time RT-PCR (qRT-PCR) assays were performed using SYBR Green Realtime PCR Master Mix (Thermo Fisher Scientific) on an Eppendorf Real-time PCR System Mastercycler RealPlex. qRT-PCR reactions were carried out with gene-specific primers (Table S1). The PCR conditions included incubation at 95 °C for 1 min followed by 40 cycles of 95 °C for 15 s, 60 °C for 20 s, and 72 °C for 30 s. A 10-fold serial dilution of pooled cDNAs was used as the template to generate a standard curve. The mRNA measurements were quantitated in three independent biological replicates and normalized to the *Bmrp49* mRNA.

2.6. RNA-seq and data analysis

Illumina sequencing analysis was performed on three biological replicates. Total RNA was isolated from *Bmix* mutant and the WT wing disc on the fifth day of fifth instar stage using TRIzol (Invitrogen), and the residual DNA was removed by incubation with RNase-free DNase I (New England BioLabs) for 30 min at 37 °C. RNA-seq libraries were constructed from 20 μg of the total RNA from each sample using the Illumina kit. The mRNA was enriched using oligo (dT) magnetic beads. The samples were mixed with the fragmentation buffer, and the mRNA reduced to short fragments (~200 bp). The first strand of the cDNA was synthesized using random hexamer primers. Buffer, dNTPs, RNase H, and DNA polymerase I were added to synthesize the second strand. The double-stranded cDNA was purified with magnetic beads. End repair and 3′-end single nucleotide adenine addition were performed. Finally, sequencing adaptors were ligated to the fragments. The fragments were enriched by PCR amplification. An Agilent 2100 Bioanaylzer and an ABI Step One Plus Real-Time PCR System were used to quantify libraries.

The library products were sequenced using an Illumina HiSeq 2000 (BGI Biotech Co. Ltd.). The raw sequencing data were qualified, filtered, and mapped to the reference silkworm genome database (http://silkworm.genomics.org.cn/) using tophat/bowtie2. The UniGene abundances were measured in fragments per kb of exon per million fragments mapped (FPKM). The differentially expressed genes were annotated functionally using Gene Ontology and Kyoto Encyclopedia of Genes and Genomes annotations.

2.7. Statistics

Experimental data were analyzed with Student's t-test (*, $P < 0.05$; **, $P < 0.01$; ***, $P < 0.001$). At least three independent replicates were used for each treatment, and data are reported as means ± standard errors of the mean (SEM).

3. Results

3.1. Bmix is predominantly expressed during the early pupal stage

It was previously reported that in *B. mori ix* is expressed in many tissues, and a testis-specific splice form has been detected although the functional significance is unknown (Arunkumar and Nagaraju, 2011). In *Drosophila*, *ix* is a single-exon gene that is not sex-specifically spliced. Analysis of Flybase showed that *Dmix* is highly expressed in the gonad, wing disc, and leg disc. We investigated spatial and temporal expression patterns of *Bmix* in 11 tissues at the wandering stage using qRT-PCR. *Bmix* mRNA was detected in all tissues studied with highest levels observed in the gonad, midgut, epidermis, and fatbody (Fig. 1A). We further analyzed *Bmix* mRNA levels in the gonad and wing disc from day 1 of fifth instar larvae (L5D1) to day 6 of the pupal stage (P6). *Bmix* mRNA levels in wing disc dissected from larvae were low but began to increase from day 2 of the prepupal stage (PP2). During the pupal stages, *Bmix* mRNA levels in the wing disc reached the maximum at P2 and decreased again at P3 and P5 (Fig. 1B). These data suggested that *Bmix* is ubiquitous and peaks early in the pupal stage.

3.2. Targeted mutagenesis of Bmix using a transgene-based CRISPR/Cas9 system

We used a binary transgenic CRISPR/Cas9 system designed to target exons 1 and 4 of *Bmix* to create silkworms with reduced levels of *Bmix* (Fig. 2A). In the system used, one *piggyBac*-based transformation vector contains the Cas9-nuclease open reading frame driven by the silkworm *nanos* promoter (nos-Cas9) as previously reported (Xu et al., 2017a). The gene encoding enhanced green fluorescent protein (EGFP) driven by the *IE1* promoter serves as a marker gene. A second transformation vector encodes the sgRNA driven by the silkworm U6 promoter and the DsRed2 fluorescent marker gene under control of the *IE1* promoter (Fig. 2B). The nos-Cas9 and three independent U6-sgRNA parental transgenic lines were established separately and crossed with each other to obtain F_1 founder moths. The *Bmix* mRNA levels were decreased to 58%, 67%, and 45% in the mutant animal relative to WT levels (Fig. 2C). Characterization of the somatic mutations by PCR using gene-specific primer pairs indicated that both male and female animals had mutations at the target site caused by non-homologous end joining-induced indels and that most of these were deletions (Fig. 2D and E).

3.3. Bmix is critical for female sex differentiation

The *ix* gene is essential for proper development of the female external genital in *D. melanogaster* (Garrett-Engele et al., 2002). Therefore, we first investigated the adult external characteristics in the *Bmix* mutants. Normal sex-specific adult external characteristics include a ventral chitin plate and genital papilla in females and claspers in males; all are essential for copulation. In *Bmix*-ablated adult females, the ventral plate was absent, and genital papilla and ventral chitin plate had severe morphological abnormalities, similar to those of the

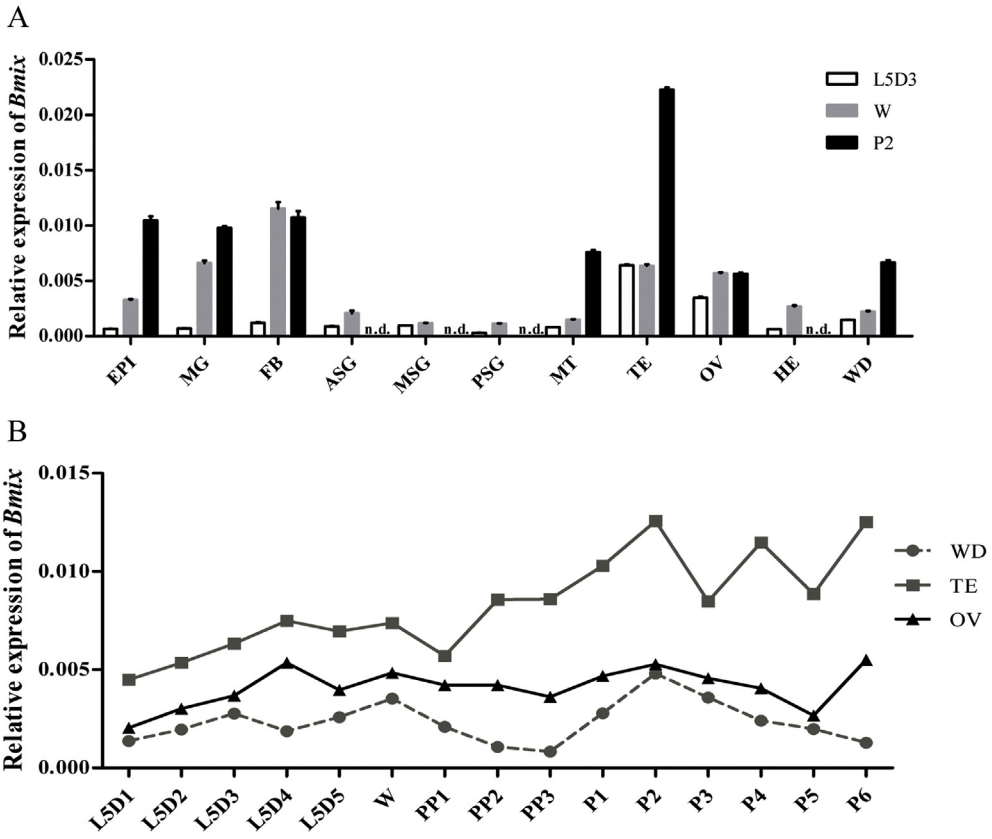

Fig. 1. Spatial and temporal expression of *Bmix*. (**A**) The relative mRNA levels of *Bmix* in epidermis (Epi), midgut (MG), fat body (FB), anterior silk gland (ASG), middle silk gland (MSG), posterior silk gland (PSG), Malpighian tubule (MT), testis (TE), ovary (OV), head (HE), and wing disc (WD) were determined by qRT-PCR. Three representative stages, day three of the fifth instar (L5D3), wandering (W), and day 2 of the pupal stage (P2) were sampled. The data shown are means ± SEM. (n = 3). (**B**) The mRNA levels of *Bmix* in WD, Te, and Ov from day one of the fifth instar (L5D1) to day six of the pupal stage (P6).

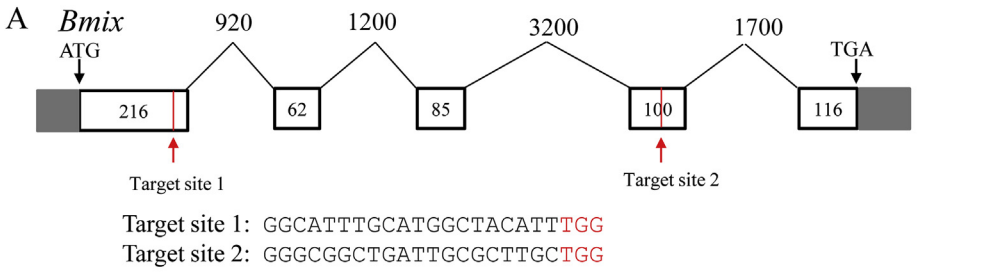

Fig. 2. Targeting *Bmix* gene using a binary transgenic CRISPR/Cas9 system. (**A**) The gene structure of the *Bmix*. Gray boxes indicate 5′- and 3′-UTRs, and white boxes indicate coding exons. Numerals indicate number of nucleotides. Target sites 1 and 2 are the sites targeted by sgRNA. (**B**) Schematics of the binary transgenic vectors used to target Cas9 to *Bmix*. (**C**) The transcript levels of *Bmix* in three lines *Bmix* mutant lines. The asterisks indicate the significant differences ($P < 0.001$) compared with the relevant control with a two-tailed *t*-test. Plotted are means ± SEM. (**D**) Somatic mutations were induced in the F_1 founder animals following crosses of nos-Cas9 and U6-sgRNA strains. A region of 2000 bp encompassing the *Bmix* locus revealed deletion events in the G_0 mutants. The red arrowhead indicates the shorter fragment present in the mutants. (**E**) Sequences of the targeted region in the *Bmix* locus in the heterozygous offspring after crossing nos-Cas9 and U6-BmixsgRNA transgenic silkworm lines. The PAM sequence is in red. The numbers of nucleotides deleted in each line are indicated to the right. (For interpretation of the references to colour in this figure legend, the reader is referred to the Web version of this article.)

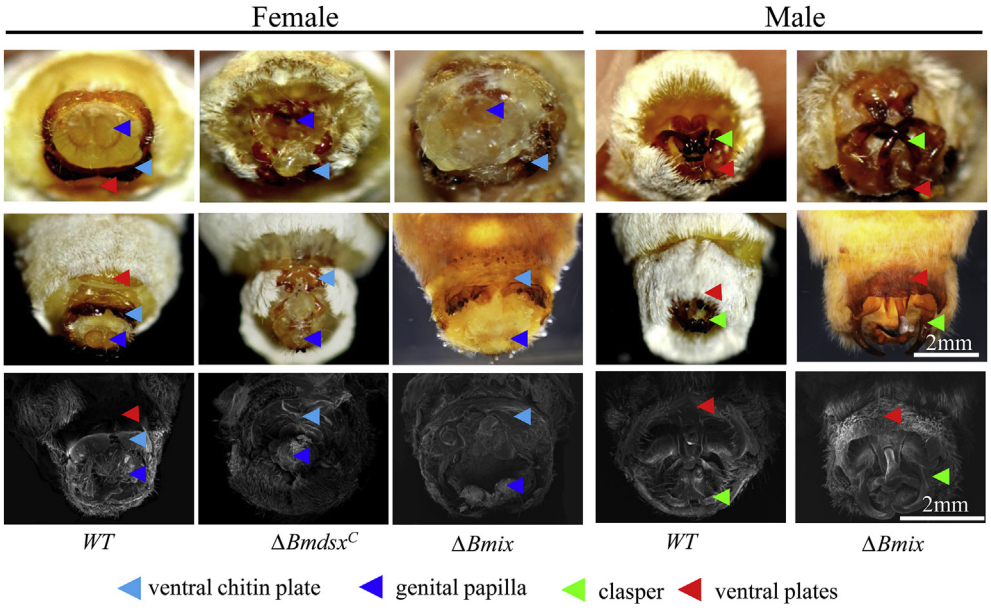

Fig. 3. Female external genitalia of *Bmix* mutant insects are abnormal. Lateral view (upper panel) and front view (middle and lower panels) of external genitalia of WT, $Bmdsx^C$, and *Bmix* individuals. The WT female external genitalia consist of a ventral chitin plate, genital papilla, and ventral plate. The WT adult male external genitalia consist of claspers and a ventral plate. The ventral chitin plate of the external genitalia of the *Bmix* mutant female is similar to that of the $Bmdsx^C$ mutant. The *Bmix* mutant males have normal external genitalia. The blue arrows indicate the ventral chitin plate, the purple arrows indicate the genital papillae, the green arrows denote the claspers, and the red arrows indicate the ventral plates. (For interpretation of the references to colour in this figure legend, the reader is referred to the Web version of this article.)

previously reported $Bmdsx^C$ (common region of *Bmdsx* gene) mutant females (Fig. 3, Xu et al., 2017b). Like the $Bmdsx^C$ mutant females, the *Bmix* mutant females are sterile is this because females are not able to copulate with males due to abnormal genital structures. The *Bmix*-ablated adult males have normal appearing external genitals (Fig. 3). *Bmix* mutant males were still sterility due to abnormal development of antenna, eye and wing, these apparatuses were essential for the male moth courtship and mating (Fig. 5).

3.4. *Bmix functions independently of Bmdsx*

Considering the phenotypic similarities between the *Bmix* and *Bmdsx* mutant females, we evaluated the splicing pattern of the *Bmdsx* gene in the *Bmix* mutants. This analysis showed that reduced levels of *Bmix* in the whole body had no effect on the splicing of *Bmdsx* gene (Fig. 4A). The gonads in the *Bmix* mutants were normal (Fig. 4B). These data indicate that the *Bmix* regulates female external genital development but not internal genital development. In *D. melanogaster*, IX interacts with DSX^F to regulate female external genital development and

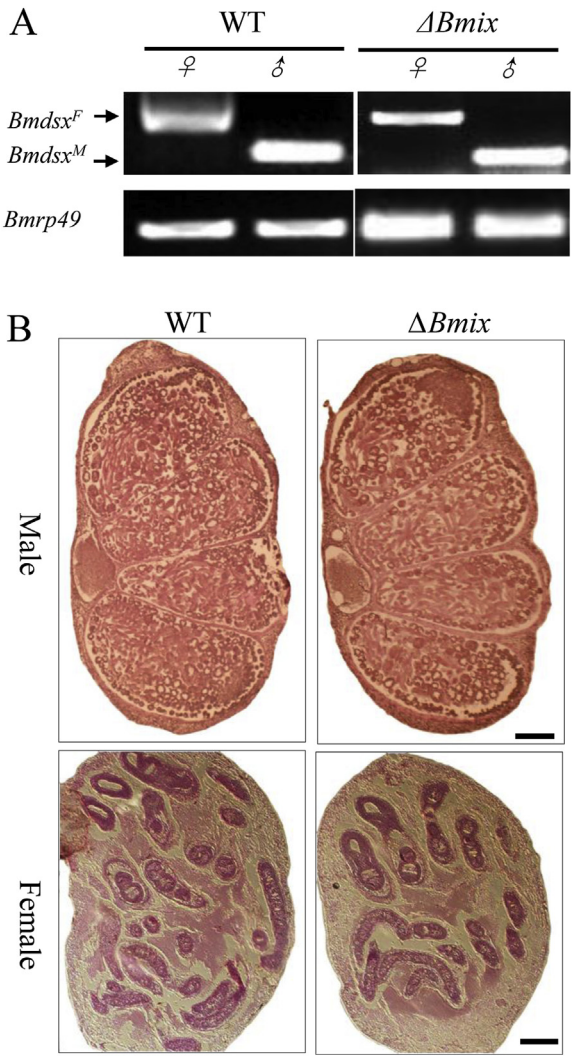

Fig. 4. *Bmix* performing function independent with *Bmdsx*. (**A**) *Bmdsx* splicing was analyzed in *Bmix* mutants and WT insects. $Bmdsx^F$ and $Bmdsx^M$ are the female- and male-specific splicing isoforms of *Bmdsx*, respectively. The lower panel shows amplification of the *rp49* transcript, which served as an internal control for RNA extraction and RT-PCR. (**B**) Morphologies of internal gonad structures in paraffin sections stained with hematoxylin and eosin; gonads were dissected from WT and mutant males and females on the fourth day of the fifth-instar. Scale bars: 200 μm.

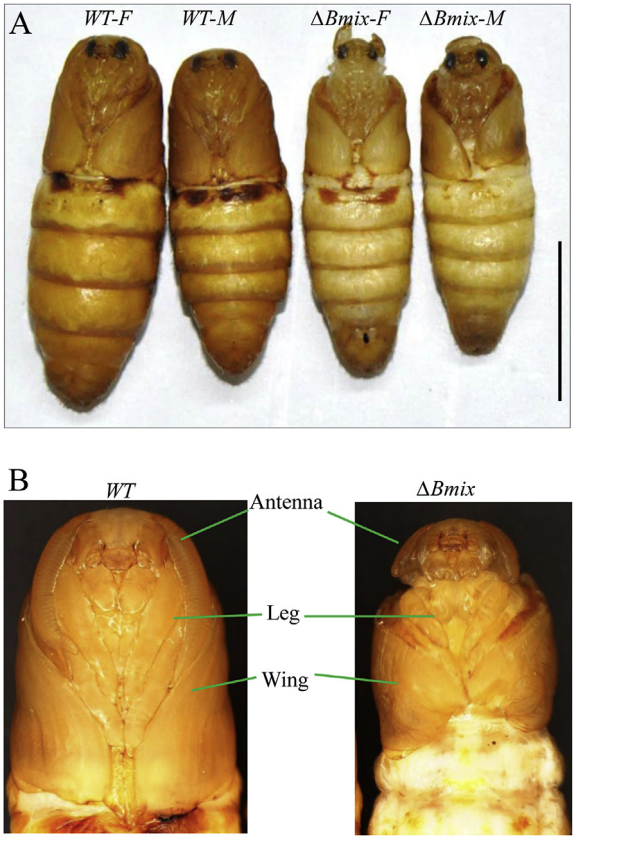

Fig. 5. Imaginal disc development is abnormal in *Bmix* mutant insects. (**A**) Gross morphology of the WT and the *Bmix* mutant insects at the pupal stage. (**B**) Loss of *Bmix* alters organogenesis of imaginal disc including wing, antenna, and leg.

also the development of internal genital (Garrett-Engele et al., 2002). In a yeast two-hybrid assay we did not detect an interaction between BmIX and $BmDSX^F$ (data not shown). These suggested that *Bmix* functions independently of *Bmdsx*.

3.5. *Bmix* is required for development of the wing imaginal disc

The *Bmix* mutant silkworms had no obvious abnormalities in egg production, viability, sex ratio, or metamorphosis. The *Bmix* mutant silkworms had abnormalities in antenna, leg, and wing formation during the pupal transformation in both sexes; these three organs were smaller than those of the WT controls (Fig. 5). Moreover, in the *Bmix* mutant the compound eyes, which are normally composed of regularly arranged hexagons, were disordered and appeared cracked (Fig. 6A-D′). In mutants, the feathered antenna did not develop normally and had a staghorn structure (Fig. 6E-H').

The silkworm has a pair of meso- and meta-thoracic discs located laterally in larvae. These discs evert during the prepupal stage of metamorphosis, and the nascent wings form outside the pupal body. The wing buds expand and inflate during adult eclosion and give rise to the corresponding fore- and hind-wings of the adult (Kango-Singh et al., 2001; Matsunaga and Fujiwara, 2002; Sato et al., 2008). The wing discs of late 5th instar *Bmix* mutant larvae were small and appeared poorly developed with veins that failed to extend from the base of the discs and that lacked tracheal invasion (Fig. 7A). Both larval and adult wing margins were irregular in morphology. The male individuals were occurred the same situation as in the female individuals (data not shown).

As these organs develop from the imaginal disc, we next to evaluated gene expression in wing discs of wandering stage *Bmix*-mutant and WT silkworms. We identified 327 differentially expressed genes: 226 genes including *Bmix* were downregulated and 101 were upregulated. KEGG enrichment analysis revealed that genes implicated in systemic lupus erythematosus, alcoholism, ECM-receptor interactions, fat digestion and absorption, cell adhesion, and focal adhesion were enriched in the differentially expressed genes (Fig. 7B). As confirmed by qRT-PCR, the levels of transcripts of genes known to be related to wing disc development, *Bmawd*, *Bmfng*, *Bmwnt1*, and *Bmyki* were significantly downregulated, whereas *BmHh* and *BmHpo* were significantly upregulated (Fig. 7C). We previously demonstrated that knockout of *Bmawd* or *Bmfng* caused wing defect phenotypes and down-regulation of *Bmwnt1* mRNA (Ling et al., 2015).

4. Discussion

Here we evaluated the biological function of the *ix* gene in the model lepidopteran insect *B. mori*. The *Bmix* transcript is ubiquitously expressed. Levels peak in the early pupal stages. We used transgenic-based CRISPR/Cas9 to delete sequence from the *Bmix* locus. The *Bmix* female mutants had abnormal external genitalia resulting in sterility,

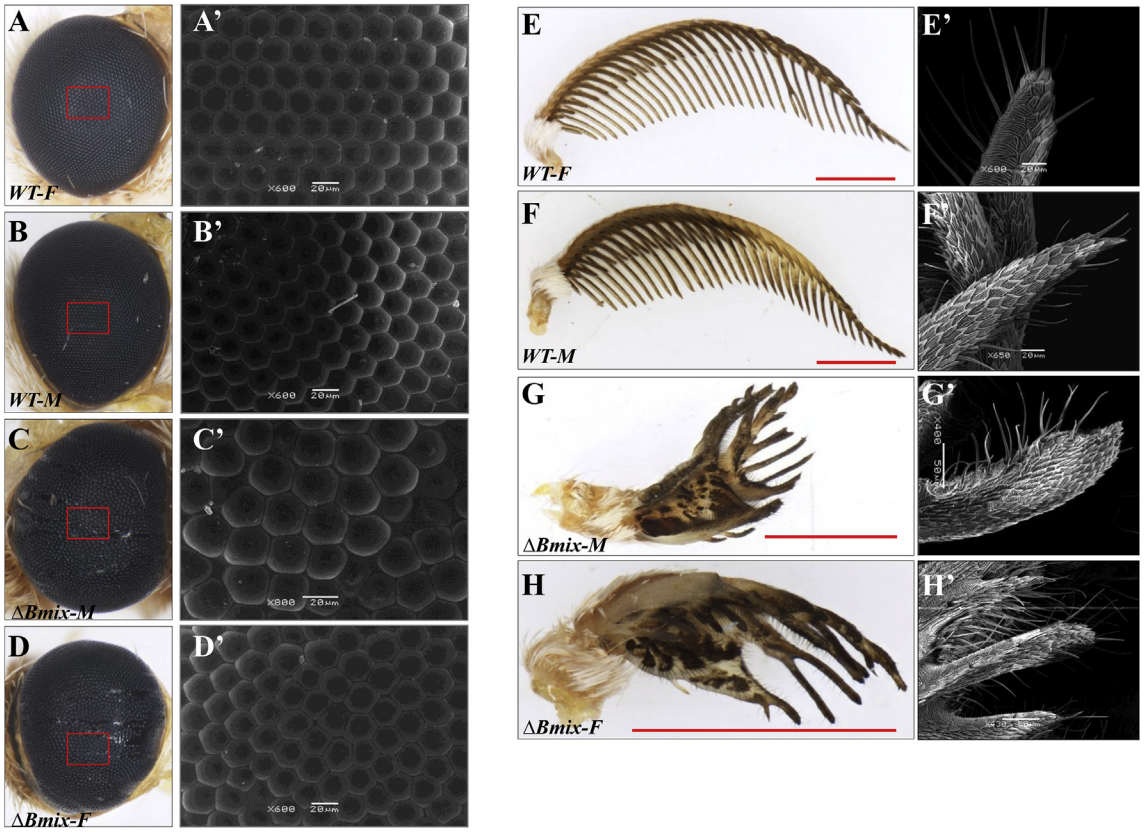

Fig. 6. Eye and antenna of *Bmix* mutants are abnormal. (**A-D**) Photographs of eyes of WT and *Bmix* mutant males and females taken under normal light. (**A′-D′**) Scanning electron microscopy images of the regions in red boxes in panels A-D. Scale bars: 20 μm. (**E-H**) Photographs of WT and *Bmix* mutant antenna taken under normal light. Scale bars: 1 mm. (**E′-H′**) Scanning electron microscopy images of antenna surface structures. Scale bars: 20 μm. (For interpretation of the references to colour in this figure legend, the reader is referred to the Web version of this article.)

whereas the male mutant external genitalia were normal. Development of the imaginal disc was abnormal in both male and female *Bmix* mutants. RNA-seq analyses showed that genes involved in WNT, HIPPO, and HEDGEHOG signaling pathways and wing development genes *Bmawd* and *Bmfng* were differentially expressed in the *Bmix* mutants compared with wild-type animals.

In *Drosophila*, activation of *Hh* signaling induces transcription of target genes *wnt*, *dpp*, and *ptc* (Hsia et al., 2017; Teleman and Cohen, 2000; Bangi and Wharton, 2006; Barrio and Milán, 2017; Callejo et al., 2008). In *Drosophila* wing imaginal discs, this response occurs exclusively in anterior (A) compartment cells, whereas *Hh* is produced and secreted exclusively in posterior (P) compartment cells from where it spreads toward the A compartment (Basler and Struhl, 1994). Interfering with expression of these genes in the wing imaginal disc results in abnormal morphology (Bangi and Wharton, 2006; Barrio and Milán, 2017; Hartl and Scott, 2014). In *B. mori*, loss of *Bmfng* function reduces *Bmwnt1* transcript levels in *flügellos* mutants and in *Bmfng* knockout individuals (Sato et al., 2008; Ling et al., 2015). We speculate that the imaginal disc defects we observed in the *Bmix* mutant silkworms are caused by dysregulation of the *Hh* and the *wnt* signaling pathways. In support of this, we detected high levels of *Bmix* at early in the pupal stage, which is when the imaginal disc develops.

Our previous study focus on the *Bmdsx* and revealed that sex-specific splicing has the oppose function on the sexual organs morphogenesis (Xu et al., 2017b). The C-terminal region (CTR) is characteristic of the products of the insect DM domain genes and they have relatively high rates of evolution (Eirín-López and Sánchez, 2015). This variation through splicing may provide the basis for the evolution of sex-specific effects on the expression of the gene isoforms. We suspected that the *Bmdsx* and *Bmix* might occur the functional evolution in the silkworm.

The results of this study clearly show that *Bmix* is involved not only in normal development of female external genitalia but also regulates imaginal disc morphogenesis, which has not been reported previously. These functions of *Bmix* in the silkworm demonstrate functional gain during evolution. Future study will focus on how *Bmix* affects imaginal disc development at specific stages. Moreover, manipulating *Bmix* may be useful for developing novel methods to control lepidopteron pests as it may enable establishment of a sex-specific sterile strain or a flightless moth to permit genetic sexing.

Authors' contributions

J.X. and Y.P.H. conceived and designed the experiments. J.X., Y.Y., and K.C. performed experiments. J.X., Y.Y., K.C., and Y.P.H. analyzed the data. J.X. wrote the manuscript and all the authors approved the final version of the manuscript prior to submission.

Conflicts of interest

We declare we have no competing interests.

Funding

This work was supported by grants from the National Science Foundation of China (31530072, 31420103918, and 31572330) and the Strategic Priority Research Program of Chinese Academy of Sciences (XDB11010500) to Y.P.H. J.X. was supported by the National Science Foundation of China (31802005), the National Postdoctoral Program for Innovative Talents (BX201700268), and the China Postdoctoral Science Foundation (2017M621548). The authors

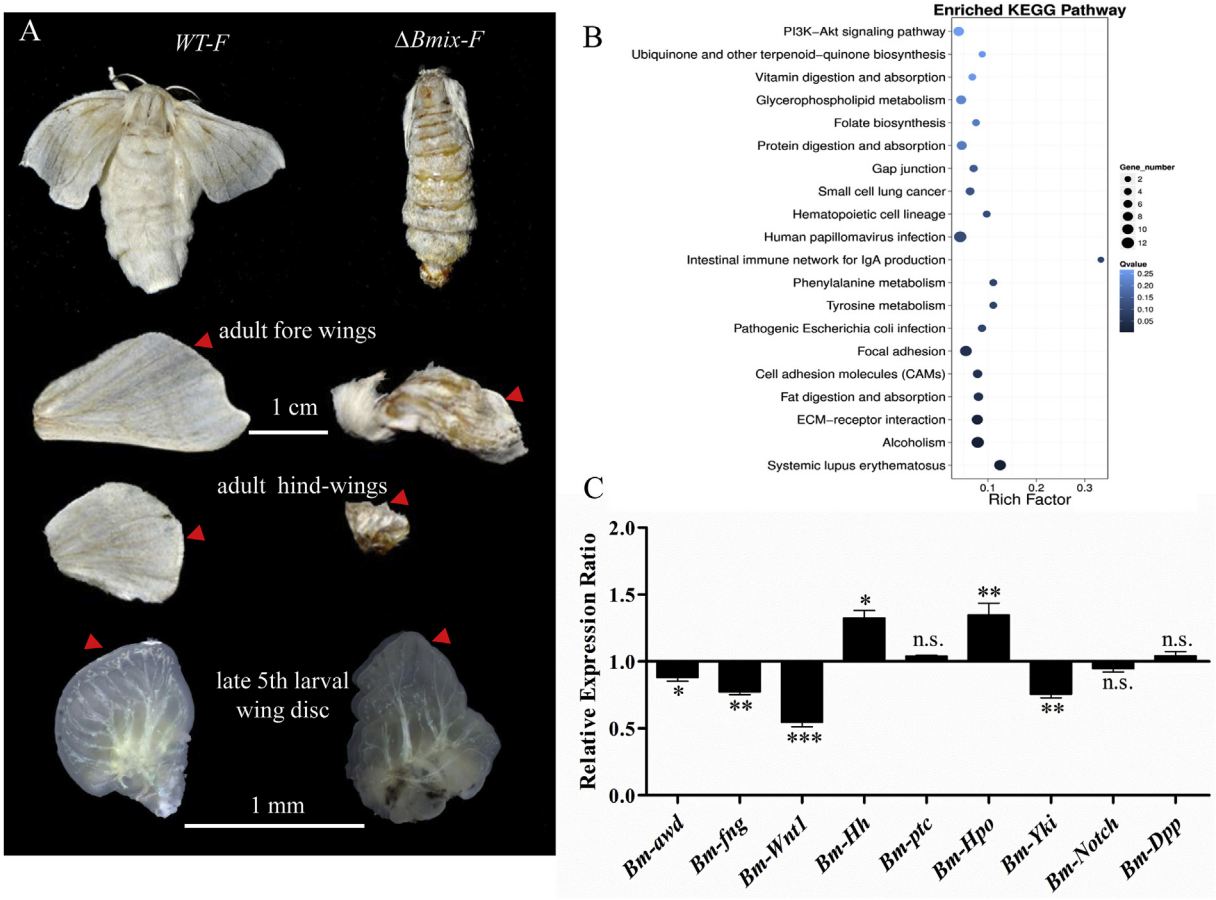

Fig. 7. *Bmix* loss-of-function causes developmental defects in the wing morphogenesis. (**A**) Photographs of wings of *Bmix* mutant and WT females at the late 5th larval instar stage. The fore- and hind-wings of *Bmix* mutants are curled and margins are irregular, and veins are disordered and atrophied (red arrowheads). (**B**) KEGG pathways enriched in genes differentially expressed in imaginal discs of *Bmix* mutants compared to WT. Log2 fold change more than or equal to 5 and $p < 0.05$ were used as the cutoff criteria. (**C**) Relative expression of indicated transcripts in wing imaginal discs of *Bmix* mutants compared to WT determined by qRT-PCR. The asterisks indicate the significant differences (*P < 0.05; **P < 0.01; ***P < 0.001) compared with the relevant control with a two-tailed *t*-test. Plotted are means ± SEM. (For interpretation of the references to colour in this figure legend, the reader is referred to the Web version of this article.)

gratefully acknowledge the support of SA-SIBS scholarship program.

Acknowledgements

We thank Jiqin Li and Xiaoyan Gao for TEM technique supports. We thank all members of the Huang lab for technical assistance and helpful discussions. We would like to thank Jacqueline Wyatt for proofreading the manuscript.

Appendix A. Supplementary data

Supplementary data to this article can be found online at https://doi.org/10.1016/j.ibmb.2019.02.003.

References

Arunkumar, K.P., Nagaraju, J., 2011. Drosophila *intersex* orthologue in the silkworm, *Bombyx mori* and related species. Genetica 139, 141–147.
Bangi, E., Wharton, K., 2006. Dpp and Gbb exhibit different effective ranges in the establishment of the BMP activity gradient critical for *Drosophila* wing patterning. Dev. Biol. 295, 178–193.
Barrio, L., Milán, M., 2017. Boundary Dpp promotes growth of medial and lateral regions of the *Drosophila* wing. Elife 6, e22013.
Basler, K., Struhl, G., 1994. Compartment boundaries and the control of *Drosophila* limb pattern by Hedgehog protein. Nature 368, 208–214.
Burtis, K.C., Baker, B.S., 1989. Drosophila *doublesex* gene controls somatic sexual differentiation by producing alternatively spliced mRNAs encoding related sex-specific polypeptides. Cell 56, 997–1010.
Callejo, A., Culi, J., Guerrero, I., 2008. Patched, the receptor of Hedgehog, is a lipoprotein receptor. Proc. Natl. Acad. Sci. U. S. A 105, 912–917.
Cavaliere, D., Di Cara, F., Polito, L.C., Digilio, F.A., 2009. Cloning and functional characterization of the *intersex* homologous gene in the pest lepidopteron *Maruca vitrata*. Int. J. Dev. Biol. 53, 1057–1062.
Chatterjee, R.N., Chatterjee, P., Kuthe, S., Acharyya-Ari, M., Chatterjee, R., 2015. *Intersex (ix)* mutations of *Drosophila melanogaster* cause nonrandom cell death in genital disc and can induce tumours in genitals in response to *decapentaplegic* (dpp^{disk}) mutations. J. Genet. 94, 207–220.
Eirín-López, J.M., Sánchez, L., 2015. The comparative study of five sex-determining proteins across insects unveils high rates of evolution at basal components of the sex determination cascade. Dev. Gene. Evol. 225, 23–30.
Erickson, J.W., Quintero, J.J., 2007. Indirect effects of ploidy suggest X chromosome dose, not the X:A ratio, signals sex in *Drosophila*. PLoS Biol. 5, e332.
Garrett-Engele, C.M., Siegal, M.L., Manoli, D.S., Williams, B.C., Li, H., Baker, B.S., 2002. *intersex*, a gene required for female sexual development in Drosophila, is expressed in both sexes and functions together with *doublesex* to regulate terminal differentiation. Development 129, 4661–4675.
Gempe, T., Beye, M., 2011. Function and evolution of sex determination mechanisms, genes and pathways in insects. Bioessays 33, 52–60.
Graham, P.L., Yanowitz, J.L., Penn, J.K., Deshpande, G., Schedl, P., 2011. The translation initiation eIF4E regulates the sex-specific expression of the master switch gene *Sxl* in *Drosophila melanogaster*. PLoS Genet. 7, e1002185.
Hsia, E.Y.C., Zhang, Y., Tran, H.S., Lim, A., Chou, Y.H., Lan, G., Beachy, P.A., Zheng, X., 2017. Hedgehog mediated degradation of Ihog adhesion proteins modulates cell segregation in *Drosophila* wing imaginal discs. Nat. Commun. 8, 1275.
Hall, A.B., Basu, S., Jiang, X., Qi, Y., Timoshevskiy, V.A., Biedler, J.K., Sharakhova, M.V., Elahi, R., Anderson, M.A., Chen, X.G., Sharakhov, I.V., Adelman, Z.N., Tu, Z., 2015. A male-determining factor in the mosquito *Aedes aegypti*. Science 348, 1268–1270.
Hartl, T.A., Scott, M.P., 2014. Wing tips: the wing disc as a platform for studying Hedgehog signaling. Methods 68, 199–206.
Hashiyama, K., Hayashi, Y., Kobayashi, S., 2011. *Drosophila Sex lethal* gene initiates female development in germline progenitors. Science 333, 885–888.
Kango-Singh, M., Singh, A., Gopinathan, K.P., 2001. The wings of *Bombyx mori* develop from larval discs exhibiting an early differentiated state: a preliminary report. J.

Biosci. 26, 167–177.
Kappes, G., Deshpande, G., Mulvey, B.B., Horabin, J.I., Schedl, P., 2011. The *Drosophila Myc* gene, *diminutive*, is a positive regulator of the *Sex-lethal* establishment promoter, *Sxl-Pe*. Proc. Natl. Acad. Sci. U.S.A. 108, 1543–1548.
Kiuchi, T., Koga, H., Kawamoto, M., Shoji, K., Sakai, H., Arai, Y., Ishihara, G., Kawaoka, S., Sugano, S., Shimada, T., Suzuki, Y., Suzuki, M.G., Katsuma, S., 2014. A single female-specific piRNA is the primary determiner of sex in the silkworm. Nature 509, 633–636.
Krzywinska, E., Dennison, N.J., Lycett, G.J., Krzywinski, J., 2016. A maleness gene in the malaria mosquito *Anopheles gambiae*. Science 353, 67–69.
Ling, L., Ge, X., Li, Z., Zeng, B., Xu, J., Chen, X., Shang, P., James, A.A., Huang, Y., Tan, A., 2015. MiR-2 family targets awd and fng to regulate wing morphogenesis in *Bombyx mori*. RNA Biol. 12, 742–748.
Matsunaga, T.M., Fujiwara, H., 2002. Identification and characterization of genes abnormally expressed in wing-deficient mutant (fl€ugellos) of the silkworm, *Bombyx mori*. Insect Biochem. Mol. Biol. 32, 691–699.
Mine, S., Sumitani, M., Aoki, F., Hatakeyama, M., Suzuki, M.G., 2017. Identification and functional characterization of the sex-determining gene *doublesex* in the sawfly, *Athalia rosae* (Hymenoptera: Tenthredinidae). Appl. Entomol. Zool. 52, 497–509.
Mysore, K., Sun, L., Tomchaney, M., Sullivan, G., Adams, H., Piscoya, A.S., Severson, D.W., Syed, Z., Duman-Scheel, M., 2015. siRNA-Mediated silencing of *doublesex* during female development of the Dengue vector mosquito *Aedes aegypti*. PLoS Neglected Trop. Dis. 9, e0004213.
Naito, Y., Hino, K., Bono, H., Ui-Tei, K., 2015. CRISPRdirect: software for designing CRISPR/Cas guide RNA with reduced off-target sites. Bioinformatics 31, 1120–1123.
Sakai, H., Sumitani, M., Chikami, Y., Yahata, K., Uchino, K., Kiuchi, T., Katsuma, S., Aoki, F., Sezutsu, H., Suzuki, M.G., 2016. Transgenic expression of the piRNA-Resistant *Masculinizer* gene induces female-specific Lethality and partial female-to-male sex Reversal in the silkworm, *Bombyx mori*. PLoS Genet. 12, e1006203.
Sato, K., Matsunaga, T.M., Futahashi, R., Kojima, T., Mita, K., Banno, Y., Fujiwara, H., 2008. Positional cloning of a *Bombyx wingless* locus *flugellos* (*fl*) reveals a crucial role for fringe that is specific for wing morphogenesis. Genetics 179, 875–885.
Siegal, M.L., Baker, B.S., 2005. Functional conservation and divergence of *intersex*, a gene required for female differentiation in *Drosophila melanogaster*. Dev. Gene. Evol. 215, 1–12.
Sharma, A., Heinze, S.D., Wu, Y., Kohlbrenner, T., Morilla, I., Brunner, C., Wimmer, E.A., van de Zande, L., Robinson, M.D., Beukeboom, L.W., Bopp, D., 2017. Male sex in houseflies is determined by *Mdmd*, a paralog of the generic splice factor gene *CWC22*. Science 356, 642–645.
Shukla, J.N., Palli, S.R., 2012. Doublesex target genes in the red flour beetle, *Tribolium castaneum*. Sci. Rep. 2, 948.
Suzuki, M.G., Suzuki, K., Aoki, F., Ajimura, M., 2012. Effect of RNAi-mediated knockdown of the *Bombyx mori transformer-2* gene on the sex-specific splicing of *Bmdsx* pre-mRNA. Int. J. Dev. Biol. 56, 693–699.
Teleman, A.A., Cohen, S.M., 2000. *Dpp* gradient formation in the *Drosophila* wing imaginal disc. Cell 103, 971–980.
Vicoso, B., Bachtrog, D., 2013. Reversal of an ancient sex chromosome to an autosome in *Drosophila*. Nature 499, 332–335.
Wang, Y., Li, Z., Xu, J., Zeng, B., Ling, L., You, L., Chen, Y., Huang, Y., Tan, A., 2013. The CRISPR/Cas System mediates efficient genome engineering in *Bombyx mori*. Cell Res. 23, 1414–1416.
Xu, J., Chen, S., Zeng, B., James, A.A., Tan, A., Huang, Y., 2017a. *Bombyx mori P-element Somatic Inhibitor* (*BmPSI*) is a key auxiliary factor for silkworm male sex determination. PLoS Genet. 13, e1006576.
Xu, J., Wang, Y., Li, Z., Ling, L., Zeng, B., James, A.A., Tan, A., Huang, Y., 2014. Transcription activator-like effector nuclease (TALEN)-mediated female-specific sterility in the silkworm, *Bombyx mori*. Insect Mol. Biol. 23, 800–807.
Xu, J., Zhan, S., Chen, S., Zeng, B., Li, Z., James, A.A., Tan, A., Huang, Y., 2017b. Sexually dimorphic traits in the silkworm, *Bombyx mori*, are regulated by *doublesex*. Insect Biochem. Mol. Biol. 80, 42–51.